input), or CED-12 (~2% of input), bound to GST-PSR-1-IN but not to the GST protein alone (Fig. 3B). Thus, PSR-1 appears to interact specifically with CED-5 and CED-12. The intracellular domain of human PSR also bound CED-5 and CED-12, albeit its binding to CED-5A was weaker (fig. S2). These results are consistent with the observation that human PSR can partially rescue the engulfment defect of the *psr-1* mutant. We investigated which region of PSR-1-IN bound CED-5 and CED-12 and found that a C-terminal deletion (amino acids 135 to 257) in PSR-1-IN greatly reduced the binding of PSR-1-IN to both CED-5 and CED-12 (Fig. 3C). Expression of a PSR-1 protein containing this deletion in the *psr-1(tm469)* mutant did not rescue the engulfment defect (Table 1), suggesting that the binding of PSR-1 to CED-5 and CED-12 may be important for the activity of *psr-1* and that PSR-1 may act through CED-5 and CED-12 to promote cell corpse engulfment.

Phagocytosis of apoptotic cells is an integral part of cell death execution and an important event in tissue remodeling, suppression of inflammation, and regulation of immune responses (*25*, *26*). Our observations indicate that *C. elegans* PSR-1, a PS-binding receptor, is important for cell corpse engulfment in vivo and likely transduces the engulfment signal through the CED-5 and CED-12 signaling pathway to promote cell corpse engulfment. However, PSR-1 appears unlikely to be the only engulfment receptor in the *ced-5* and *ced-12* signaling pathway, because the *psr-1* mutant has a weaker engulfment defect than do any of the *ced-2*, *ced-5*, *ced-10*, or *ced-12* mutants. Identification of other engulfment receptors that also act through the *ced-5* and *ced-12* signaling pathway will help to address the fundamental question of how apoptotic cells are recognized and phagocytozed during apoptosis.

References and Notes

1. V. A. Fadok *et al.*, *J. Immunol.* **149**, 4029 (1992).
2. R. F. Ashman, D. Peckham, S. Alhasan, L. L. Stunz, *Immunol. Lett.* **48**, 159 (1995).
3. S. J. Martin *et al.*, *J. Exp. Med.* **182**, 1545 (1995).
4. B. Verhoven, R. A. Schlegel, P. Williamson, *J. Exp. Med.* **182**, 1597 (1995).
5. I. Vermes, C. Haanen, H. Steffens-Nakken, C. Reutelingsperger, *J. Immunol. Methods* **184**, 39 (1995).
6. S. M. van den Eijnde *et al.*, *Cytometry* **29**, 313 (1997).
7. S. M. van den Eijnde, L. Boshart, C. P. M. Reutelingsperger, C. I. De Zeeuw, C. Vermeij-Keers, *Cell Death Differ.* **4**, 311 (1997).
8. S. Krahling, M. K. Callahan, P. Williamson, R. A. Schlegel, *Cell Death Differ.* **6**, 183 (1999).
9. A. Shiratsuchi, S. Osada, S. Kanazawa, Y. Nakanishi, *Biochem. Biophys. Res. Commun.* **246**, 549 (1998).
10. P. R. Hoffmann *et al.*, *J. Cell Biol.* **155**, 649 (2001).
11. V. A. Fadok *et al.*, *Nature* **405**, 85 (2000).
12. V. A. Fadok, A. de Cathelineau, D. L. Daleke, P. M. Henson, D. L. Bratton, *J. Biol. Chem.* **276**, 1071 (2001).
13. Materials and methods are available as supporting material on *Science* Online.
14. J. Parrish *et al.*, *Nature* **412**, 90 (2001).
15. X. C. Wang, D. Xue, unpublished results.
16. L. C. Cheng, Y. C. Wu, unpublished results.
17. Z. Zhou, E. Hartwieg, H. R. Horvitz, *Cell* **104**, 43 (2001).
18. R. E. Ellis, D. M. Jacobson, H. R. Horvitz, *Genetics* **129**, 79 (1991).
19. Y. C. Wu, M. C. Tsai, L. C. Cheng, C. J. Chou, N. Y. Weng, *Dev. Cell* **1**, 491 (2001).
20. Z. Zhou, E. Caron, E. Hartwieg, A. Hall, H. R. Horvitz, *Dev. Cell* **1**, 477 (2001).
21. T. L. Gumienny *et al.*, *Cell* **107**, 27 (2001).
22. Y. C. Wu, H. R. Horvitz, *Nature* **392**, 501 (1998).
23. P. W. Reddien, H. R. Horvitz, *Nature Cell Biol.* **2**, 131 (2000).
24. E. Brugnera *et al.*, *Nature Cell Biol.* **4**, 574 (2002).
25. J. Savill, V. Fadok, *Nature* **407**, 784 (2000).
26. P. M. Henson, D. L. Bratton, V. A. Fadok, *Curr. Biol.* **11**, R795 (2001).
27. T. Nakano *et al.*, *J. Biol. Chem.* **272**, 29411 (1997).
28. V. Fadok, unpublished results.
29. J. E. Sulston, E. Schierenberg, J. G. White, J. N. Thomson, *Dev. Biol.* **100**, 64 (1983).

30. We thank M. Han, Y. Kohara, and Z. Zhou for reagents and strains; M. Valencia and V. Zapata for help with statistical analysis; and B. Wood and L. Edgar for help with four-dimensional microscopy analysis. This research was supported in part by the Searle Scholar Award and the Burroughs Wellcome Fund Career Award (D.X.), and grants from the Ministry of Education (89-B-FA01-1-4) and National Science Council of Taiwan (Y.-C.W.); the Ministry of Education, Culture, Sports, Science and Technology of Japan (S.M.); and NIH (D.X. and V.A.F.).

Supporting Online Material

www.sciencemag.org/cgi/content/full/302/5650/1563/DC1
Materials and Methods
Figs. S1 and S2
References

5 June 2003; accepted 8 October 2003

Fish Exploiting Vortices Decrease Muscle Activity

James C. Liao,[1]* David N. Beal,[2] George V. Lauder,[1] Michael S. Triantafyllou[2]

Fishes moving through turbulent flows or in formation are regularly exposed to vortices. Although animals living in fluid environments commonly capture energy from vortices, experimental data on the hydrodynamics and neural control of interactions between fish and vortices are lacking. We used quantitative flow visualization and electromyography to show that trout will adopt a novel mode of locomotion to slalom in between experimentally generated vortices by activating only their anterior axial muscles. Reduced muscle activity during vortex exploitation compared with the activity of fishes engaged in undulatory swimming suggests a decrease in the cost of locomotion and provides a mechanism to understand the patterns of fish distributions in schools and riverine environments.

Many fishes live in habitats in which they commonly encounter vortices that arise from fluid flow past stationary objects or from the propulsive movements of other animals. Energy extraction from environmental vortices has been consistently implicated as a hydrodynamic mechanism to increase the performance of swimming fishes (*1*–*8*). The preference of fishes to use these unsteady flows has been documented in the field (*4*, *9*, *10*) and laboratory (*11*–*13*). However, the dynamic and transparent nature of flowing water has precluded quantitative visualization of interactions between fishes and vortices and, thus, an understanding of the underlying physical mechanisms involved. Furthermore, the effect of vortical flows on the degree and pattern of axial muscle activity in fishes remains entirely unknown.

We generated periodic vortices of similar strength and size to each other by using a vertically mounted D-section cylinder (i.e., a cylinder bisected along its long axis) placed in water flowing at a known velocity (*14*) (Fig. 1). These vortices were shed from the D-section cylinder in a staggered array collectively known as a Kármán street (*15*). A Kármán street is an example of a drag wake (rotation of alternately shed vortices is toward each other upstream), which can form between the thrust wakes (rotation of alternately shed vortices is toward each other downstream) of two fish swimming side by side (*5*). Vortices generated by the D-section cylinder were similar in strength to those produced by other freely swimming fish (*16*, *17*).

Compared with swimming in free stream (uniform) flow, there are two hydrodynamic benefits of station holding behind a cylinder. Fish can simply swim against the current in the region of reduced flow, drafting, for example, as a bicyclist would behind another bicyclist, or they can generate lift to move against the flow by altering their body kinematics to synchronize with the shed vortices. Because energy can be captured from cylinder vortices (*18*), trout that synchronize their body kinematics to vortices appropriately may need to use very little energy and, thus, gain a hydrodynamic advantage beyond that of drafting in the reduced velocity alone.

[1]Department of Organismic and Evolutionary Biology, Harvard University, Cambridge, MA 02138, USA. [2]Department of Ocean Engineering, Massachusetts Institute of Technology, Cambridge, MA 02139, USA.

*To whom correspondence should be addressed: E-mail: jliao@oeb.harvard.edu

Simultaneous visualization of a two-dimensional, horizontal slice through the columnar vortices generated by the D-section cylinder (*15*) using digital particle image velocimetry (DPIV) (*19*) and the movements of trout with high-speed video (Fig. 1) revealed that trout slalom between vortices rather than through them (Fig. 2, A and B; Movie S1). If the flow is decomposed into a downstream (*x* axis, Fig. 1) and a lateral (*z* axis) component, slaloming between vortices occurs when trout move against the downstream flow but with the local lateral flow. Slaloming through oncoming vortices requires opposing the local lateral flow. Actuated foils generate more thrust if they slalom through rather than between Kármán vortices (*20*), but they require more power input to oppose the instantaneous local flow. Trout slalom between rather than through vortices and, thus, minimize power input rather than maximize thrust output. To quantify the movement of trout near vortices, we described the phase relation between the lateral motions of points along the body relative to the arrival of drifting vortices (Fig. 2C). When the center of a vortex drifted down to the center of mass (COM) of the fish, the COM was at its maximum lateral excursion away from the vortex, indicated by a phase relation of 180°. For all points anterior to the COM, the body moved away from an oncoming vortex (<180°), whereas body points posterior to the COM move toward the vortex (>180°). A phase relation of 0° or 360° would indicate that the fish had intercepted the center of a vortex.

In their preferred position holding station, one to two body lengths (*L*) downstream from the cylinder and away from the low-pressure suction region (*15*), trout synchronize their tail-beat frequency to the vortex shedding frequency of the cylinder and display large lateral body movements (Fig. 3, A and C). These kinematic features characterize a mode of locomotion termed the Kármán gait (*11*). This pattern of movement qualifies as a gait based on previous definitions applied to moving animals, in which body kinematics are observed to change discontinuously (*21*, *22*), usually across a range of speeds or environments. Trout that adopt the Kármán gait display a body wavelength (a description of body shape based on a sine wave) that is longer than the cylinder wake wavelength (downstream spacing of vortices, Fig. 3B). This resulted from the head interacting differently with a vortex than did the tail (Fig. 2C), and ensures that the incident flow is maintained at an angle to the body to generate lift (*23*, *24*). Due to buffeting caused by cylinder vortices, the lateral body motion was much greater than for fish swimming in the free stream (Fig. 3C). Body kinematics have a consistent relation with the frequency and phase of the vortex wake across several cylinder treatments (*11*), which supports our hypothesis that trout can extract energy from the wake in addition to benefiting from drafting in the reduced flow behind the cylinder. Other fishes with a diversity of body shapes and occupying different ecological niches (brook trout, *Salvelinus fontinalis*; alewives, *Alosa pseudoharengus*; bluegill sunfish, *Lepomis macrochirus*; and yellow perch, *Perca flavescens*) also exhibited the Kármán gait.

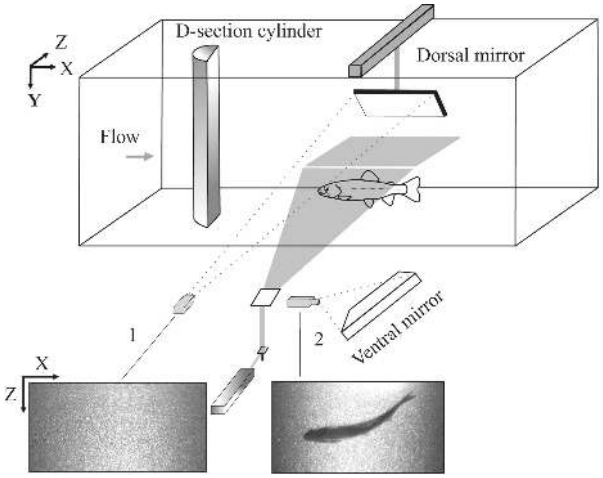

Fig. 1. Experimental setup to simultaneously visualize columnar vortices shed from a D-section cylinder (using DPIV; camera 1) and the body kinematics of station-holding trout (camera 2).

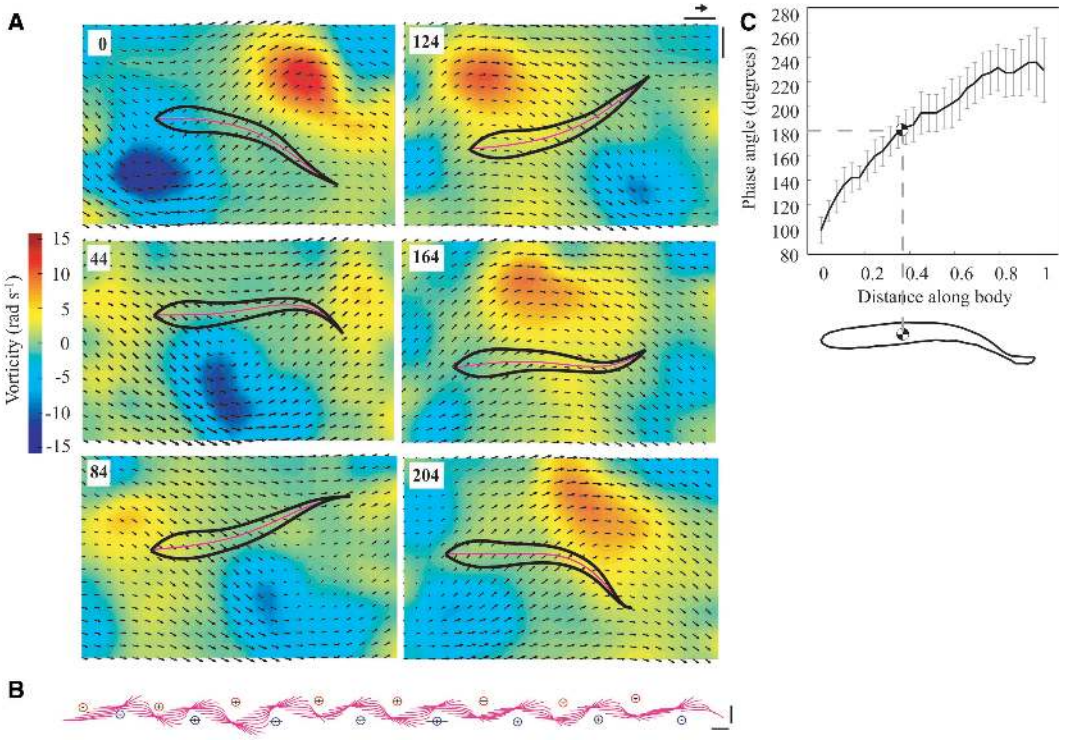

Fig. 2. Interaction of trout with cylinder vortices. Scale bars represent 2 cm. (**A**) Time series (ms) of body outlines (black) and midlines (purple) superimposed onto vorticity and velocity vector plots of the cylinder wake. Arrows indicate flow direction and magnitude (scale arrow = 56 cm s^{-1}). Red and blue represent clockwise and counterclockwise vorticity (radians per second), respectively. (**B**) Midlines for seven consecutive tail-beats, beginning from right to left, of which (A) is a subset. Standard errors in vortex position given as bar lengths within each vortex. (**C**) Phase between body and vortices, where 180° represents slaloming in between vortices and 0° or 360° represents vortex interception. Fish center of mass shown as checkered circles. Standard error bars are in light gray.

Little is known about muscle activity patterns for fish swimming in perturbed environments. Using fine wire electrodes to record electrical muscle activity, we found that trout only activated their anterior, axial red muscles when they adopted the Kármán gait (Fig. 4B). This pattern of isolated muscle activity represents a fundamental departure from the pattern of propagating muscle activity characteristic of propulsive, undulatory locomotion (Fig. 4A) (*25*–*27*), and further lends support for identifying this mode of locomotion as a distinct gait (*22*). Isolated, anterior muscle activity during the Kármán gait demonstrates that drafting (i.e., undulatory propulsion in reduced flow) is not the sole mechanism for station holding behind a cylinder. Image analysis of stereotypic body positions during separate DPIV and electromyography experiments illustrates that anterior red muscles become active on the opposite side of the body before a vortex reaches the COM (Fig. 4B). Anterior muscle activity may serve to modulate the angle of attack of the head and body, functioning to sustain body orientation or initiate changes in yaw. Thus, trout can hold station behind a cylinder in fast, downstream flow by recruiting relatively few muscles to control their body orientation to exploit oncoming vortices instead of recruiting most of their axial muscles to generate thrust via undulation. The small amount of muscle activity seen during the Kármán gait is perhaps not surprising, given that even passive hydrofoils can generate thrust when synchronized to an oscillating flow (*23*, *24*).

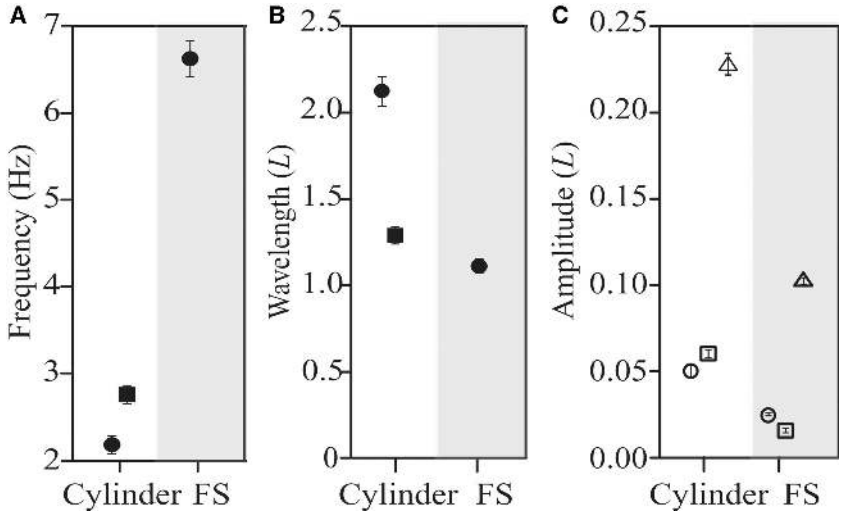

Fig. 3. Comparison of body kinematics (filled circles) with associated wake variables (filled squares) in the presence of a D-section cylinder and in the absence of a D-section cylinder, or free stream flow (FS). Error bars are shown but may be obscured by data symbols. (**A**) Tail-beat frequencies for trout behind a cylinder and in the free stream, along with the vortex-shedding frequency of the cylinder. (**B**) Body wavelength for trout behind the cylinder and in the free stream, along with the cylinder wake wavelength (where *L* is total body length). (**C**) Lateral body amplitudes, where open circles, squares, and triangles represent the snout, center of mass, and tail tip, respectively.

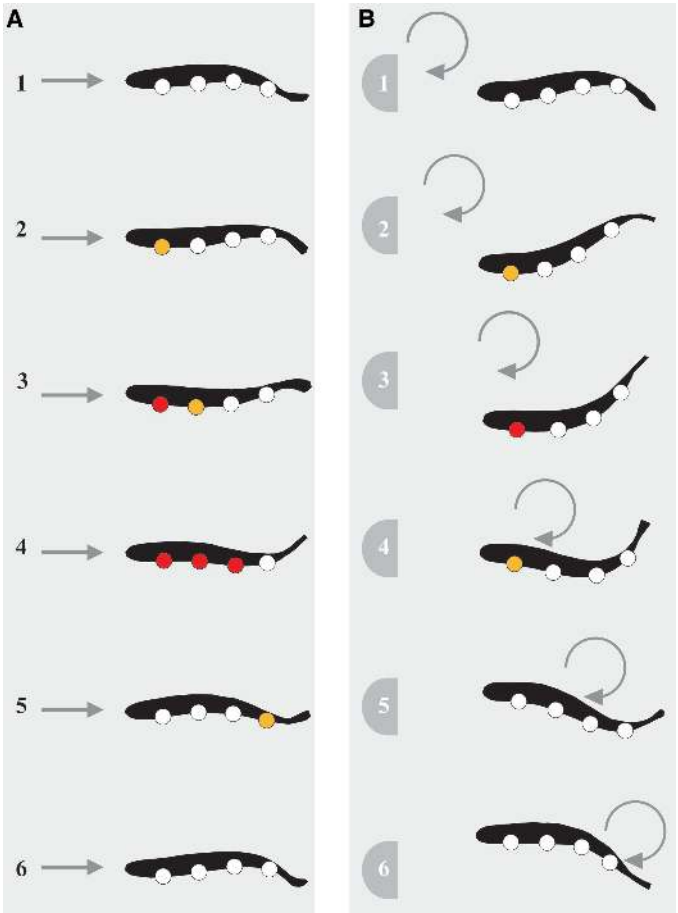

Fig. 4. Time series illustrating that axial red muscle activity differs between trout swimming in free stream flow versus trout holding station behind a cylinder. Circles denote electrode positions with no (open), intermediate (orange), or high (red) muscle activity. (**A**) A propagating wave of muscle activity for a trout swimming in the free stream. (**B**) Muscle activity for a trout behind a D-section cylinder with estimated locations of a clockwise vortex.

Our results show a mechanism by which swimming fish can use environmental vortices, which is likely to reduce the cost of locomotion. In a turbulent environment, use of the Kármán gait allows the body of a fish to act as a self-correcting hydrofoil. Design of foil propulsors for biomimetic autonomous underwater vehicles could benefit from the reduced power costs associated with the self-adjusting motions of the Kármán gait. Demonstrating a link between vortex interaction and reduced muscle activity may also provide insight into the dynamics and evolution of aggregation in moving animals. Although trout behind a cylinder slalom in between vortices, vortex interception, although previously discounted (*28*), can, in theory, facilitate upstream acceleration and explain temporary deviations from the optimal pattern of school formation (*5*, *29*). In addition, a precise understanding of the interactions between muscle activity and vortices across species promises to aid in the design and implementation of fish passageways.

References and Notes

1. J. Herskin, J. F. Steffensen, *J. Fish. Biol.* **53**, 366 (1998).
2. S. I. Hartwell, R. G. Otto, *Trans. Am. Fish. Soc.* **107**, 793 (1978).
3. K. Streitlien, G. S. Triantafyllou, *AIAA (Am. Inst. Aeronaut. Astronaut.) J.* **34**, 2315 (1996).
4. S. G. Hinch, P. S. Rand, *Can. J. Fish. Aquat. Sci.* **57**, 2470 (2000).
5. D. Weihs, *Nature* **241**, 290 (1973).
6. C. M. Breder, *Zoologica* **50**, 97 (1965).
7. V. V. Belyayev, G. V. Zuyev, *Prob. Ichthyol.* **9**, 578 (1969).
8. M. V. Abrahams, P. W. Colgan, *Environ. Biol. Fishes* **20**, 79 (1987).
9. D. S. Pavlov, A. I. Lupandin, M. A. Skorobogatov, *J. Ichthyol.* **40**, S232 (2000).
10. K. D. Fausch, *Can. J. Fish. Aquat. Sci.* **50**, 1198 (1993).
11. J. C. Liao, D. N. Beal, G. V. Lauder, M. S. Triantafyllou, *J. Exp. Biol.* **206**, 1059 (2003).

12. P. W. Webb, *J. Exp. Biol.* **201**, 2403 (1998).
13. T. J. Pitcher, B. L. Partridge, C. S. Wardle, *Science* **194**, 963 (1976).
14. Materials and methods are available as supporting online material on *Science* Online.
15. M. M. Zdravkovich, *Flow Around Circular Cylinders: A Comprehensive Guide Through Flow Phenomena, Experiments, Applications, Mathematical Models, and Computer Simulations* (Oxford Univ. Press, Oxford, 1997), vol. 1.
16. J. C. Nauen, G. V. Lauder, *J. Exp. Biol.* **205**, 1709 (2002).
17. E. G. Drucker, G. V. Lauder, *Integr. Comp. Biol.* **42**, 243 (2002).
18. J. M. Anderson, thesis, Joint Program MIT/Woods Hole Oceanographic Institution (1996).
19. E. G. Drucker, G. V. Lauder, *J. Exp. Biol.* **202**, 2393 (1999).
20. R. Golpalkrishnan, M. S. Triantafyllou, G. S. Triantafyllou, D. S. Barrett, *J. Fluid Mech.* **274**, 1 (1994).
21. P. W. Webb, in *The Physiology of Fishes*, D. H. Evans, Ed. (CRC Press, Boca Raton, FL, 1998) pp. 3–21.
22. R. M. Alexander, *Physiol. Rev.* **69**, 1199 (1989).
23. N. Bose, J. Lien, *Proc. R. Soc. Lond. Ser. B* **240**, 591 (1990).
24. T. Y. Wu, A. T. Chwang, in *Swimming and Flying in Nature*, T. Y.-T. Wu, C. J. Brokaw, C. Brennen, Eds., (Plenum, New York, 1975), vol. 2.
25. B. C. Jayne, G. V. Lauder, *J. Comp. Physiol.* **175**, 123 (1994).
26. L. Hammond, J. Altringham, C. Wardle, *J. Exp. Biol.* **201**, 1659 (1998).
27. S. M. McGlinchey, K. A. Saporetti, J. A. Forry, J. A. Pohronezny, D. J. Coughlin, *Comp. Biochem. Physiol.* **129**, 727 (2001).
28. C. M. Breder, *Fish. Bull.* **74**, 471 (1976).
29. B. L. Partridge, T. J. Pitcher, *Nature* **279**, 418 (1979).
30. We thank A. A. Biewener, M. A. Daley, and F. A. Jenkins Jr. for helpful comments on the manuscript. Support was provided by grants from Sigma Xi and the American Museum of Natural History to J.C.L., NSF to G.V.L., and a Massachusetts Institute of Technology Sea Grant to M.S.T.

Supporting Online Material
www.sciencemag.org/cgi/content/full/302/5650/1566/DC1
Materials and Methods
Movie S1

20 June 2003; accepted 2 September 2003

Genetic Analysis of a High-Level Vancomycin-Resistant Isolate of *Staphylococcus aureus*

Linda M. Weigel,[1]* Don B. Clewell,[2] Steven R. Gill,[3] Nancye C. Clark,[1] Linda K. McDougal,[1] Susan E. Flannagan,[2] James F. Kolonay,[3] Jyoti Shetty,[4] George E. Killgore,[1] Fred C. Tenover[1]

Vancomycin is usually reserved for treatment of serious infections, including those caused by multidrug-resistant *Staphylococcus aureus*. A clinical isolate of *S. aureus* with high-level resistance to vancomycin (minimal inhibitory concentration = 1024 μg/ml) was isolated in June 2002. This isolate harbored a 57.9-kilobase multiresistance conjugative plasmid within which Tn*1546* (*vanA*) was integrated. Additional elements on the plasmid encoded resistance to trimethoprim (*dfrA*), β-lactams (*blaZ*), aminoglycosides (*aacA-aphD*), and disinfectants (*qacC*). Genetic analyses suggest that the long-anticipated transfer of vancomycin resistance to a methicillin-resistant *S. aureus* occurred in vivo by interspecies transfer of Tn*1546* from a co-isolate of *Enterococcus faecalis*.

Staphylococcus aureus, a major cause of potentially life-threatening infections acquired in health care settings and in the community, has developed resistance to most classes of antimicrobial agents soon after their introduction into clinical use. In the late 1960s, few options were available for treatment of infections caused by strains resistant to penicillins, macrolides, aminoglycosides, and tetracyclines, a situation that led to widespread use of methicillin and other semisynthetic penicillins. However, the acquisition of genes encoding an additional penicillin-binding protein, PBP-2a, resulted in the emergence of methicillin-resistant *S. aureus* (MRSA) in many health care institutions around the world (*1*). Currently, glycopeptides such as vancomycin provide effective therapy against most strains of multidrug-resistant *S. aureus*, including MRSA (*2*).

[1]Division of Healthcare Quality Promotion, Centers for Disease Control and Prevention, Atlanta, GA 30333, USA. [2]Department of Biologic and Materials Sciences, School of Dentistry, University of Michigan, Ann Arbor, MI 48109, USA. [3]The Institute for Genomic Research, Rockville, MD 20850, USA. [4]J. Craig Venter Science Foundation Joint Technology Center, Rockville, MD 20850, USA.

*To whom correspondence should be addressed. E-mail: lweigel@cdc.gov

Resistance to vancomycin, first reported in 1988 for an isolate of *Enterococcus faecium* (*3*), is associated with one of several gene clusters, which are classified as *vanA* to *vanG* on the basis of the resulting phenotypic characteristics of the strain. The VanA phenotype, characterized by inducible, high-level resistance to vancomycin and teicoplanin, is mediated by Tn*1546* or closely related mobile genetic elements. The target of vancomycin is the carboxy terminal D-alanyl-D-alanine (D-ala-D-ala) of the disaccharide pentapeptide cell wall precursor, which is translocated by a lipid carrier to the outer surface of the cytoplasmic membrane. Enzymes encoded on the transposon replace D-ala-D-ala with a depsipeptide, D-alanyl-D-lactate (D-ala-D-lac). The affinity of vancomycin for the depsipeptide is decreased by a factor of 1000 when compared with the normal cell wall precursor terminating in D-ala-D-ala (*4*). The potential for transfer of vancomycin resistance to *S. aureus* was immediately recognized and became a major global health concern.

The first clinical isolate of *S. aureus* with decreased susceptibility to vancomycin [minimal inhibitory concentration (MIC) = 8 μg/ml] was isolated in Japan in 1997 (*5*). Additional strains have been isolated in several countries, including the United States, and are designated as vancomycin-intermediate *S. aureus* (VISA). Analysis of these isolates revealed a common structural change, a significant thickening of the cell wall (*6*). This alteration increases the number of D-ala-D-ala targets in the outer layers of the cell wall that may then "trap" the large vancomycin molecules, preventing inhibitory concentrations of the agent from reaching precursor targets before they are incorporated into the cell wall structure (*7*, *8*). Although concern for the emergence of high-level resistance was renewed, vancomycin MICs among the VISA strains remained relatively low (≤16 μg/ml). However, in June 2002 a high-level vancomycin-resistant *S. aureus* (VRSA, MIC = 1024 μg/ml vancomycin) was isolated from a dialysis patient in Michigan (*9*). This report provides a genetic analysis of the VRSA clinical isolate.

Identification of the VRSA isolate as *S. aureus* was confirmed by DNA sequence analysis of rDNA, *gyrA*, and *gyrB* (*10*). Contamination with enterococci was ruled out, because we were unable to amplify genes encoding enterococcal ligases (*11*). The *Sma*I pulsed-field gel type of the VRSA was identified as USA100 (the New York/Japan lineage) (*1*, *12*, *13*), the most common staphylococcal pulsed-field type found in U.S. hospitals.

An MIC of 1024 μg/ml of vancomycin was determined by broth microdilution (*10*). The VRSA isolate was also resistant to aminoglycosides, β-lactams, fluoroquinolones, macrolides, rifampin, and tetracycline, but was susceptible to linezolid, quinupristin/dalfopristin, and trimethoprim-sulfamethoxazole. Unlike laboratory mutants selected for vancomycin resistance, such as VM50 (*14*), the VRSA clinical isolate retained its MRSA phenotype (oxacillin MIC >128 μg/ml).

Vancomycin resistance in the VRSA isolate was identified as *vanA*-mediated by polymerase chain reaction amplification (*15*). The prototype VanA-encoding element is a 10.8-kb transposon, Tn*1546,* frequently found on plasmids in vancomycin-resistant enterococci (VRE). Therefore, we isolated plasmids from the VRSA, a co-isolate of VRE, and a vancomycin-susceptible MRSA isolated from the same patient (*10*). The VRSA harbored a single 57.9-kb plasmid, pLW1043. The MRSA contained a